CCNF-9667198

CP-9008199 - /

STI

DE 0 8 1991

LA-UR--91-14

DE91 007350

TITLE. GREEN'S FUNCTION MONTE CARLO IN NUCLEAR PHYSICS

AUTHOR(S) J. Carlson, T-5

DISCLAIMER

MASTER

Los Alamos

Los Alamos National Laboratory
Los Alamos, New Mexico 87545

FORM NO 836 R4

Green's Function Monte Carlo in Nuclear Physics

J. Carlson

T-5, MS B283, Los Alamos National Laboratory, Los Alamos, NM 87545

We review the status of Green's Function Monte Carlo (GFMC) methods as applied to problems in nuclear physics. New methods have been developed to handle the spin and isospin degrees of freedom that are a vital part of any realistic nuclear physics problem, whether at the level of quarks or nucleons. We discuss these methods and then summarize results obtained recently for light nuclei, including ground state energies, three-body forces, charge form factors and the coulomb sum. As an illustration of the applicability of GFMC to quark models, we also consider the possible existence of bound exotic multi-quark states within the framework of flux-tube quark models.

Introduction

Only within recent times has it become possible to solve realistic few-body problems accurately in nuclear physics. Although there problems have a long history (one of the first Green's function Monte Carlo applications was to s-shell nuclei[1]), the highly non-perturbative nature of the interactions, along with their strong state-dependence, kept few-body problems largely out of reach. Within the last ten years, these problems have been succesfully addressed by several computational techniques. Faddeev methods, in particular, have been very valuable in solving three-body problems. In this lecture I will address the current status of Green's function Monte Carlo (GFMC) methods as applied in nuclear physics.

I will first discuss the application of GFMC methods to light nuclei, and then review a few intriguing new results obtained in flux-tube quark models. To a large degree, the Monte Carlo techniques involved are the same, although of course different motivations underly the two areas. In light nuclei, we are interested in studying problems such as three-nucleon forces, two-body correlations and exchange currents. These calculations are all undertaken within a framework of nucleons interacting through a complicated, primarily meson-induced, interaction.

In the latter case, our goal is to obtain a qualitative understanding of the underlying field theory in the low energy and momentum regime typical of problems in nuclear physics. Toward this end, we examine flux-tube quark models which are based upon the strong-coupling limit QCD. We have recently employed GFMC techniques to study the so-called 'exotic' states in the flux-tube model; we find them to be unbound in the extreme strong-coupling limit. Many experimental searches for these particles are currently underway; for example the H particle search at Brookhaven. The presence or absence of these states experimentally may p.ovide us with information concerning the applicability of the strong-coupling limit.

Nuclear Hamiltonian & Monte Carlo Methods

First, consider solving the non relativistic Schroedinger equation for a few-body nucleus:

$$H|\Psi\rangle = \left[\sum_i -\frac{\hbar^2}{2m} \nabla_i^2 + \sum_{i<j} V_{ij} + \sum_{i<j<k} V_{ijk} + ... \right] \Psi = E|\Psi\rangle \qquad (1)$$

In this equation, the Hamiltonian is determined by fitting two- (and possibly three-) body experimental data. Clearly such a non-relativistic treatment is only a first approximation; nevertheless a great deal of physics can be examined in this way.

Variational[2] (VMC) and Green's Function Monte Carlo[1,3,4] (GFMC) methods have proven to be very valuable in the study of light nuclei. These methods have for the most part originally been developed in condensed matter physics, where they have been used to study quantum fluids and solids.[5,6] The Hamiltonian in nuclear physics is at least superficially similar to these condensed matter systems, as it consists of a very strong short-range repulsion coupled with long-range attractive terms.

The nuclear Hamiltonian, though, is complicated by the strong state-dependence of the interaction. We will concentrate chiefly on the Argonne[7] NN interaction, which may be written:

$$V_{ij} = \sum_{k,i<j} V^k(r_{ij})O^k_{ij} \tag{2}$$

where the operators O are

$$O^k_{ij} = 1, \sigma_i \cdot \sigma_j, S_{ij}, L \cdot S_{ij}, L \cdot S^2_{ij}, L^2_{ij} \tag{3}$$

multiplied by either an isospin-independent (1) or -dependent ($\tau_i \cdot \tau_j$) operator. In these expressions σ and τ represent the spin and isospin of a nucleon, S_{ij} is the tensor operator ($S_{ij} = 3\sigma_i \cdot \hat{r}_{ij}\sigma_j \cdot \hat{r}_{ij} - \sigma_i \cdot \sigma_j$), and L_{ij} is the relative angular momentum of nucleons i and j. All modern interactions (Argonne,[7] Bonn,[8] Nijmegen[9] ...) may be written in a similar manner, although the choice of non-local operators varies. These interactions consist of a one-pion interaction (which has a strong tensor component) at long distances, an intermediate range attraction, and a short-range phenomenological repulsion; they are fit to deuteron properties as well as two-body scattering data.

In a similar spirit, the three-nucleon-interaction (TNI) at long distances is assumed to have the structure of a two-pion-exchange interaction, but its precise strength is adjusted to fit the three-body binding energy.[10] The full TNI consists of the two-pion exchange piece $V_{2\pi}$ and a short-range repulsive term:

$$V_{ijk} = U_0 \sum_{cyc} W_{2\pi}(r_{ij})W_{2\pi}(r_{ik}) + A_0 \sum_{cyc} V_{2\pi}(\vec{r}_{ij}, \vec{r}_{ik}), \tag{4}$$

where the sums run over cyclic permutations of the particles, and the function $W_{2\pi}$ has the range of a two-pion interaction. The parameters U_0 and A_0 can be estimated from calculating the effects of suppressing Δ degrees of freedom, but their precise values are determined by fitting the binding energy of $A=3$ nuclei. The three-body force is quite small compared to the two-nucleon interaction, but nevertheless provides an important fraction of the total binding energy.

Variational Monte Carlo (VMC) studies of light nuclei often employ a generalized Jastrow form for the wave function:

$$|\Psi\rangle = S \left(\prod_{i<j}\right) F_{ij}|\Phi\rangle. \tag{5}$$

In this equation, Φ is an anti-symmetric Slater determinant of one-particle states, and the F_{ij} are pair correlation operators:

$$F_{ij} = f^c(r_{ij}) \left[1 + u_1 \left(\sum_k u^k(r_{ij})O^k_{ij}\right)\right] \tag{6}$$

which include the most important spin-isospin operators in the Hamiltonian. The operators for different pairs do not commute, so we introduce the symmetrization operator S to obtain an overall anti-symmetric wave function. The pair correlations are obtained by solving two-body differential equations of the general form:

$$[-\frac{\hbar^2}{m}\nabla^2 + v(r) + \lambda(r)]F = 0,$$
(7)

where the function λ contains several variational parameters. The u_3 correlation in equation 6 is a three-body term which reduces the strength of the operator-dependent two-body correlations for some configurations of the nucleons.[2] The complete wave function Ψ is constructed to have the correct asymptotic properties as one nucleon is separated from the system.

The straightforward variational Monte Carlo algorithm is limited to treating small systems, optimistically up to $A \approx 8$. For the spin-independent interactions in condensed matter physics, it is possible to simulate one to two hundred particles. For the interactions of interest in nuclear physics, however, the problems are much more complex. The wave function of a nucleus consists of $2^A\frac{A!}{N!Z!}$ spin-isospin components, the first factor represents the spin (up or down for each nucleon) and the second the isospin. These states are explicitly summed in light nuclei.

This wave function (Eq. 5) is adequate for many purposes, yielding ground state energies within a few per cent of the Faddeev values for A=3. It also gives similar results for the electromagnetic form factors.[11] Further improvements are possible by including $L \cdot S$ correlations and three-body terms.[12] For other purposes, though, especially for the study of three nucleon interaction terms in the Hamiltonian, it is necessary to develop exact methods.

Since we are interested in projecting out the ground state of the system, GFMC methods offer an attractive method for determining the exact solution. The ground state is projected through:

$$|\Psi_0\rangle = \lim_{\tau \to \infty} \exp(-H\tau)|\Psi_T\rangle,$$
(8)

where $|\Psi_T\rangle$ is an initial trial state, for example the Jastrow wave function described above. In general one cannot compute $\exp(-H\tau)$, but by dividing the propagation time τ into many small steps $\Delta\tau$:

$$\exp(-H\tau) = \prod_1^n \exp(-H\Delta\tau) = \int G(\vec{R}_n, \vec{R}_{n-1})....G(\vec{R}_1, \vec{R}_0)$$
(9)

the full propagator can be evaluated by Monte Carlo. In practice, one must use several time steps $\Delta\tau$ and extrapolate to $\Delta\tau = 0$ in order to eliminate time step errors associated with the non-commuting nature of the kinetic and potential terms. Since the potential is not merely a number here, but takes on different values in various spin-isospin channels, it is not clear how to implement the exact sampling schemes used for state-independent potential problems in atomic and condensed-matter physics. A state-independent potential can be incorporated into an equation for the exact Green's function as a probability for absorption, and hence used to terminate a random walk. The fact that the potential is more complicated here means that various short-time approximations to the Green's function are valuable.[13] In our GFMC calculations, we use time steps on the order of $1 - 5 \times 10^{-4}$ MeV^{-1}, which yield very small extrapolations to zero time step.

For short propagation times $\Delta \tau$ and static potentials, the following approximation[14] to the propagator is quite useful:

$$G(\vec{R}, \vec{R}') \approx G^0(\vec{R}, \vec{R}') S \prod_{j<i} \left[\frac{g_{ji}(\vec{r}_{ji}, \vec{r}'_{ji})}{g^0_{ji}(\vec{r}_{ji}, \vec{r}'_{ji})} \right]. \tag{10}$$

In this equation, the full G for 3A coordinates is approximately given by the free particle propagator (a gaussian) times a product of all pair propagators divided by their respective free particle propagators. The simplest approximation to the ratio in equation 10 is, of course,

$$g_{ij}/g^0_{ij} = \exp[-(\Delta \tau/2)(V_{ij}(r) + V_{ij}(r'))], \tag{11}$$

where V, and consequently g_{ij}, are operators in spin-isospin space. Exponentiating the momentum-independent terms in the two-body potential is rather straightfoward; momentum-dependent and three-body terms are generally small and a linear approximation to the Green's function can be used.

In fact, we employ a generalization of this expression, using antithetic sampling techniques to sum over a variety of 'sub-paths' in order to determine the full two-body Green's function. One could also employ the methods used by Ceperley and co-workers[14] to evaluate the pair Green's function analytically. Here, though, this technique is not as valuable as in studies of bulk-helium.

There are two reasons for this difference between condensed matter and nuclear problems. First, the core repulsion in nuclear systems is comparatively soft, so that simple approximations to the two-body propagator are not as bad. In addition, the strong state-dependence of the interaction implies rather large three-body effects, since the potential acting between various pairs does not commute. Thus, equation 10 is not as effective an approximation for the full Green's function. One simple indication of the importance of three-body spin-dependent effects is the difference between Jastrow variational calculations and exact results. For the 3-body problem with central interactions, variational calculations and exact methods give ground state energies that agree within 0.02 MeV; for more realistic interactions the difference is 0.3-0.5 MeV.

Incorporating momentum-dependent interaction terms in GFMC calculations is more difficult. Realistic models of the NN interaction do contain such pieces, including $L \cdot S, L \cdot S^2, L^2$, and p^2_{ij} operators. To date, we have only been able to include the first of these operators, $L \cdot S$, successfully in the exact GFMC algorithm. The difficulties in treating the second-order derivatives term are discussed in reference 13, and are essentially due to the fact that the nucleons gain different effective masses in the different spin-isospin channels. Of course, incorporating state-independent but momentum-dependent terms is feasible. It may be feasible to employ point symmetry group methods to treat at least a few higher-order partial waves with GFMC, although the statistical errors associated with this procedure may be prohibitive.

The Argonne interaction, though, has been constructed to some degree with the idea that these terms should be small. In fact, the expectation value of the sum of these terms in light nuclei is only one to two MeV. Consequently, we solve exactly for a modified Argonne V8 (containing only the eight operators through $L \cdot S$) interaction which best approximates the full Argonne V14 model. This model reproduces the deuteron, the singlet S, and triplet P waves (with the exception of coupling to F waves) exactly. Perturbation theory is then used to estimate the difference between

the V14 and V8 models, this difference is small (0.9 MeV) in the alpha particle. Finally, we note that this Argonne V8 model is somewhat different than that used in previous calculations.[13]

Ground State Results for Light Nuclei

I will first present a new set of results for the alpha particle with the Argonne V8 NN interaction plus Urbana model 8 TNI.[15] The GFMC method converges very rapidly for the alpha particle. as demonstrated in figure 1. This figure shows the ground state energy plotted as a function of the total iteration time τ. The variational energy is shown at $\tau = 0$; the energy then quickly drops to the exact ground state energy. In fact, the plot covers only the initial part of the calculation, up to a total iteration time of 0.012 MeV^{-1}. The actual calculation includes 5 times as many iterations to generate additional statistics, the horizontal lines in the figure are statistical error bounds obtained by averaging the results between 0.024 and 0.060 MeV^{-1}. Other quantities, of course, may not converge as rapidly as the energy. In this case, the energy converges very quickly because (1) there are no bound excitations in the four-nucleon system, the lowest resonance is approximately 20 MeV above the ground state, and (2) the primary deficiencies in the wave function seem to be short-range high-energy excitations.
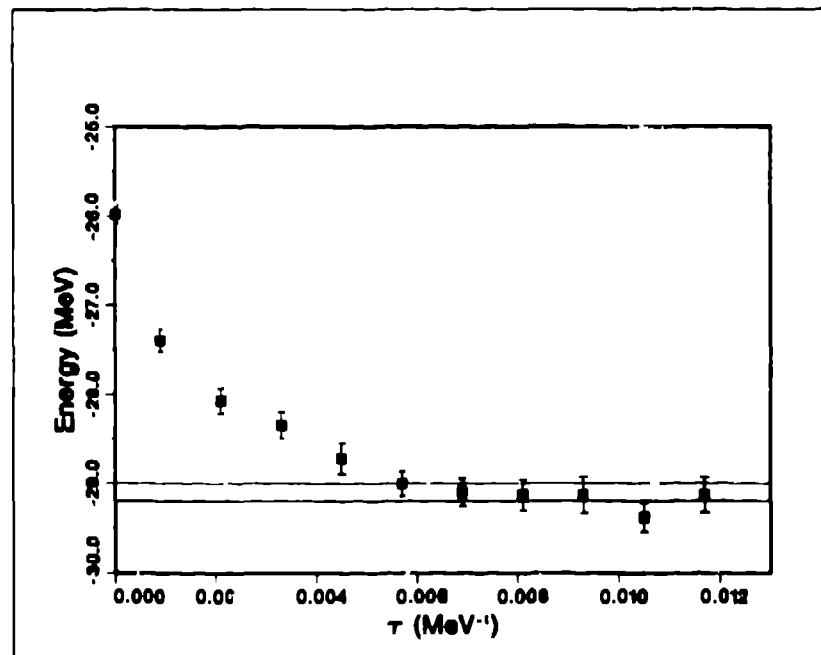

Figure 1) Alpha Particle Ground State Energy vs. iteration time τ.

We obtain a ground state energy of -29.20 ± 0.15 MeV for the Argonne V8 plus TNI model 8 interaction, approximately one MeV overbound compared to the experimental -28.3 MeV. Using first-order perturbation theory, we estimate the difference between the Argonne V14 NN interaction and the V8 model is 0.9 MeV; yielding a total energy of -28.3 $\pm$ 0.2 MeV, in remarkably good agreement with the experimental result.

Hence, it appears that the same three body force can be used to provide very accurate binding energies for three and four-body nuclei. The Urbana TNI model 8 was constructed to provide a

-8.48 MeV. The expectation value of the three nucleon interaction is a small fraction ($\leq 5\%$) of the total potential energy, so at this level there is no apparent reason to introduce four- or higher-body interaction terms. Other models (Reid, Nijmegen, ...) of the NN potential give a similar underbinding for the three- and four-body nuclei, hence it should be possible to fit the binding energies of these nuclei as well with an appropriate TNI model.

The variational wave function used in this calculation was optimized for the Argonne V14 plus Urbana model 7 TNI.[4] Consequently, it does not provide a very good estimate for the ground state energy with the model 8 TNI, which has a stronger repulsive component and a weaker two-pion-exchange term. However, the rms radius of this trial wave function is very near the exact result, hence it requires smaller extrapolations for the estimates of other properties. GFMC produces a wave function only in a statistical sense, and hence ground state energy expectation values other than the energy are extrapolated from 'mixed' and variational estimates via:

$$\langle \Psi_0 | H | \Psi_0 \rangle \approx \langle \Psi_T | H | \Psi_0 \rangle - \langle \Psi_T | O | \Psi_T \rangle. \tag{12}$$

The extrapolations required with the present variational wave function are generally quite small. The most accurate variational calculations to date[12] give a binding energy approximately one MeV higher than this GFMC calculation.
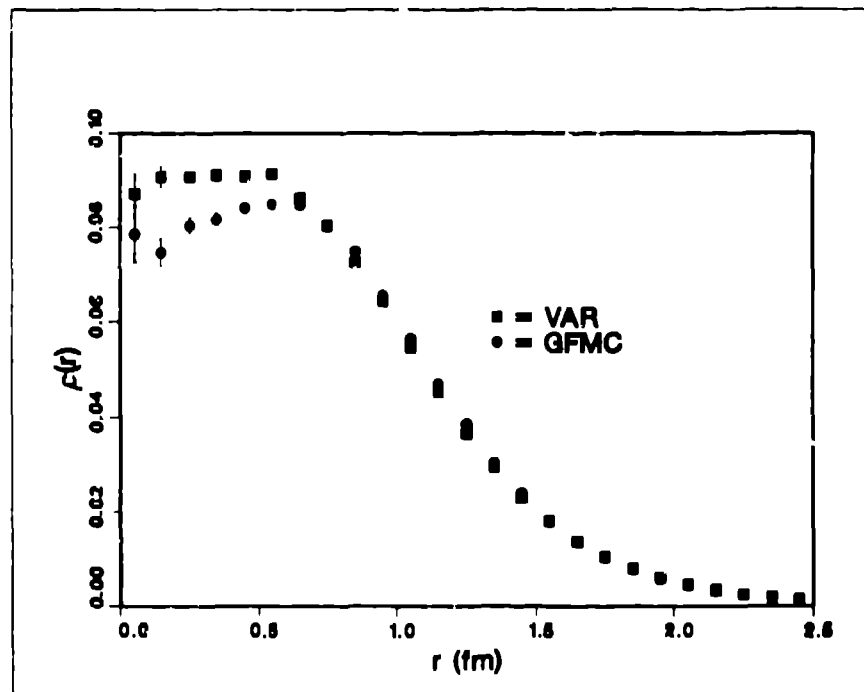

Figure 2) VMC and GFMC results for the proton density in the alpha particle.

We have also computed the proton density for both the variational and GFMC wave functions (Fig. 2). In the impulse approximation, the charge form factor of the nucleus can be obtained as the fourier transform of the one-body charge distribution. The GFMC one-body density has a slight dip in the core which does not appear in the variational results. This dip is associated with a very small region of phase space, and consequently does not affect the rms radius or charge form factor significantly at small momentum transfer. It does make a significant difference, though, in the region near and beyond the first diffraction minimum.

The effects of two-body charge and current operators can be important even at relatively low momentum transfer, and must be included when trying to make comparisons with experimental results. Since the nuclear force arises from the exchange of charged mesons, there must be two-body contributions to the charge and current operators. In particular, the importance of pion exchange currents has been know for a long time. Riska[17] has developed a method for constructing models of the exchange currents which satisfy the continuity equation:

$$\nabla \cdot \vec{j}_{ex} + i[V_{ij}, \rho] = 0 \tag{13}$$

with an arbitrary potential V_{ij}. This equation is used to constrain the 'model-independent' exchange currents. In addition, there are transverse pieces in the current (e.g. $N\Delta\gamma, \rho\pi\gamma$, and $\omega\pi\gamma$) which are not so constrained. Using this method, Schiavilla and Riska have computed the magnetic form factors of ^{3}He and ^{3}H, as well as the backward cross-section for the electrodisintegration of the deuteron. Their results a good agreement with experiment up to quite high values of momentum transfer.

They have also computed the charge form factors of the three-body nuclei,[18] and obtain good agreement with experimental results. The charge operators are more speculative since they involve relativistic corrections and are not constrained by the continuity equation. However, in the alpha particle some of the uncertainties are decreased because of the isoscalar nature of the system. We have combined the following one-body charge operator:

$$\rho_1(q) = [1 - \frac{q^2}{8m^2}]\frac{1}{2}[G_E^S(q) + G_E^V(q)\tau_z]$$
$$- i\frac{\sigma \cdot q \times P}{8m^2}\frac{1}{2}\left\{[G_E^S(q) - 2G_M^S(q)] + [G_E^V(q) - 2G_M^V(q)]\tau_z\right\}. \tag{14}$$

incorporating the Darwin-Foidy term and a small $L \cdot S$ correction, with a two-body charge operator due to pions:

$$\rho_\pi(q) = \frac{3}{2m}\{\left[F_1^S(q)\tau_i \cdot \tau_j + F_1^V(q)\tau_{jz}\right](\sigma_i \cdot q\sigma_j \cdot k_j)\bar{v}_\pi(k_j)+$$
$$\left[F_1^S(q)\tau_i \cdot \tau_j + F_1^V(q)\tau_{iz}\right](\sigma_j \cdot q\sigma_i \cdot k_i)\bar{v}_\pi(k_i)\} \tag{15}$$

to calculate the charge form factor of the alpha particle. This form of charge operator was first considered by Kloet and Tjon in examining pion photoproduction.[19] We have also included the remaining terms of Schiavilla and Riska, but their effect is an order of magnitude smaller than the terms above up to a momentum transfer of ≈ 5.5 fm^{-1}.

Figure 3 illustrates the contribution of one-body and pion-exchange terms to the charge form factor. As is apparent in the figure, the VMC and GFMC results give nearly identical results for the exchange currents. However, the one-body terms do show a significant difference in the region of the second maximum. This difference is a result of a sensitive cancellation in the fourier transform (it is down by two orders of magnitude from its value at $k = 0$) and hence small changes in density can produce large effects.
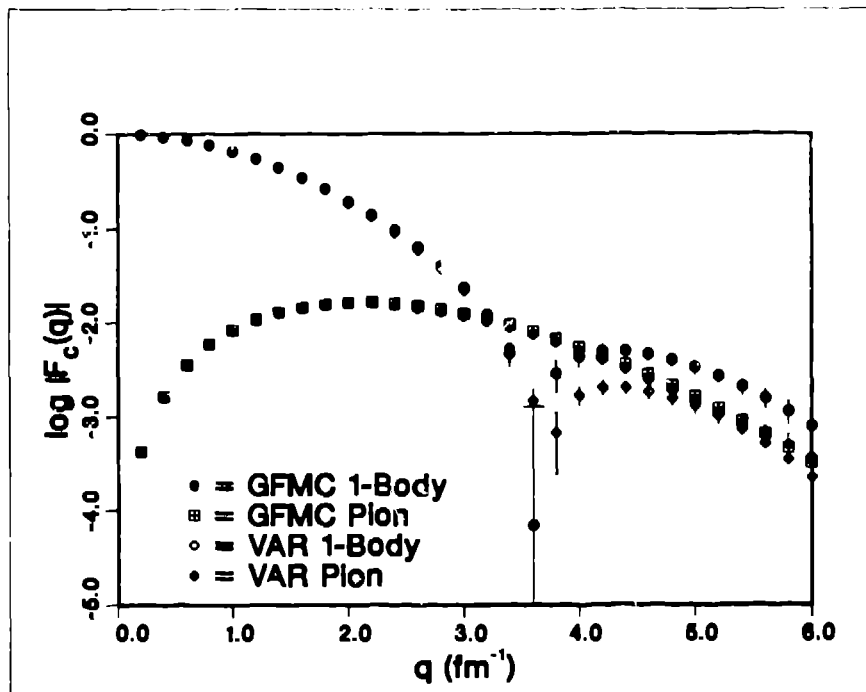
Figure 3) VMC and GFMC results for one-body and pion contributions to the alpha particle charge form factor.

The full calculations are compared to experimenta' results in figure 4. The GFMC calculation is in excellent agreement with experimental results up to a momentum transfer of ≈ 4.5 fm^{-1}. Beyond that point, the calculated form factor is significantly larger than experimental results. Nevertheless, the overall agreement is excellent, particularly at lower momentum transfers where one would expect the theory to work best.

Figure 4) Alpha particle charge form factor, experimental and calculated.

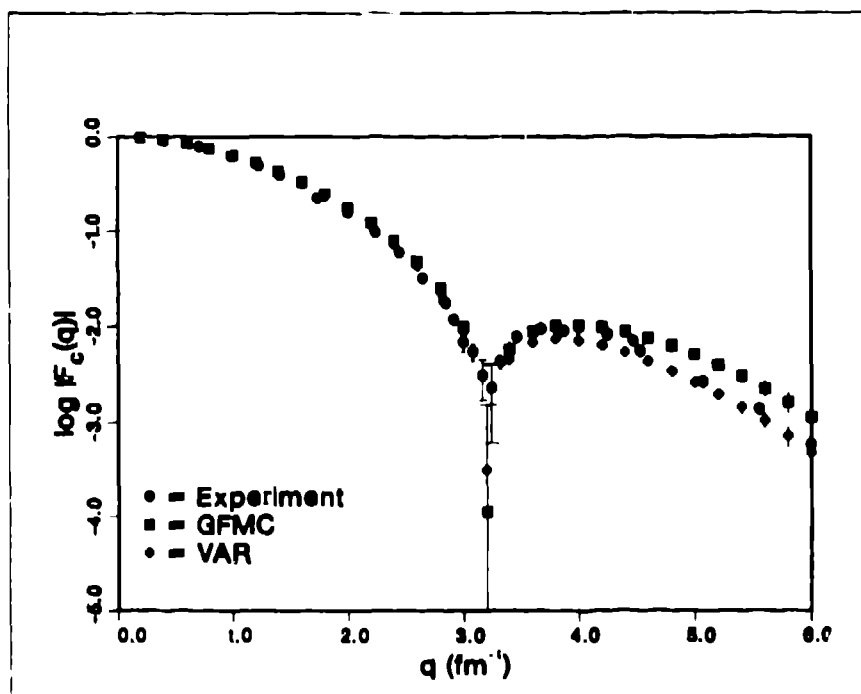The two-body distributions can also be measured to some degree with electron scattering experiments. The Coulomb sum depends upon the total inelastic cross section summed over all final states, and is defined as:

$$S = \frac{1}{Z} \int_{\omega_{el}^+}^{\infty} \frac{R_L(q,\omega)}{[G_E(q^2)]^2} d\omega,$$ (16)

where R_L is the longitudinal response of the nucleus and G_E is the proton form factor. The integral extends from energies just above elastic scattering to infinity, which allows us to use closure to calculate the Coulomb sum as a ground state expectation value.

$$S = \frac{1}{Z} \left[\langle 0| \sum_{j=1}^{A} \rho_j^\dagger(q) \sum_{k=1}^{A} \rho_k(q)|0 \rangle - \frac{[ZF_c(q^2)]^2}{[G_E(q^2)]^2} \right],$$ (17)

where

$$\rho_k(q) = \exp(iq \cdot r_k)[\frac{1 + \tau_{zk}}{2}]$$ (18)

if we ignore small neutron contributions (which are included in the calculations) and two-body terms. In this approximation, the Coulomb sum is simply:

$$S = 1 - Z\frac{[F_c(q^2)]^2}{[G_E(q^2)]^2} + \frac{1}{Z}\rho_{PP}(q),$$ (19)

where F_c is the charge form factor of the nucleus and $\rho_{pp}(q)$ is the fourier transform of the two-body distribution function integrated over the pair's center-of-mass.

Figure 5 compares the theoretical and experimental calculations. Since experiments extend only to a finite energy, they have been extrapolated using energy- and energy-squared weighted sum rules by Schiavilla et al.[20,21] using variational wave functions. The contributions of this tail region are given by the difference between the points labeled 'extr' and 'trunc'; the latter includes only the response up to the experimental limit. As shown in the figure, the VMC and GFMC curves are nearly identical, and both agree very well with the extrapolated results.
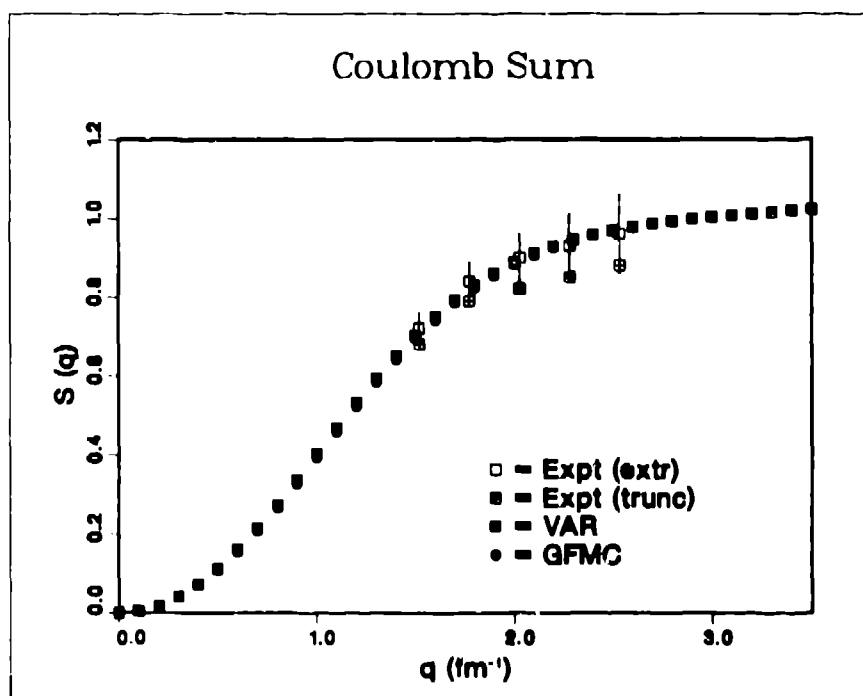

Figure 5) Coulomb sum in the alpha particle

Beck[22] extracted $\rho_{pp}(q)$ from the experimental results in the three-nucleon system using a slightly different extrapolation technique and the theoretical results for the neutron contributions. Although the qualitative features of the experimental and theoretical curves are similar, the experimental $\rho_{pp}(q)$ is much higher beyond the first minimum. This would indicate even a stronger correlation in the protons than is present theoretically, but contributions of two-body operators to the Coulomb sum should be included before strong conclusions are drawn.

We seem to have in hand a theoretical picture of light nuclei that is consistent with a wide range of nuclear properties. This picture relies upon the importance of three-body forces and also of exchange current contributions to the electromagnetic properties of light nuclei. Several avenues for future research remain open, however. In particular, the effect of relativistic dynamics may be important. This could in principle be studied with light cone methods, but little has been done to date with realistic interaction models. In addition, of course, one would like to study heavier nuclei to determine whether their properties can also be explained within a consistent scheme.

Low-Energy Scattering

The five-nucleon system is particularly interesting in this regard. Although there are no five-nucleon bound states experimentally, the $J^\pi = 1/2^-$ and $3/2^-$ states do exist as sharp low-energy resonances. In the simplest picture, these states are one-body p-wave scattering off an alpha particle core; with an $L \cdot S$ splitting describing the difference between the $J=1/2$ and $3/2$ states. These states have been studied variationally by enclosing the system within a spherical box,[23] and then matching the asymptotic wave function to the nodes at the boundaries of the box. Variational calculations of the five-body system give fair agreement with experimental results for the $1/2$ state, which is somewhat higher in energy, but indicate that the Hamiltonian is not attractive enough in the $J=3/2$ channel.

Other methods are available for extremely low-energy calculations or calculations in non-resonant channels. By specifying the logarithmic derivative at the boundary and then minimizing the energy with respect to changes in the variational wave function, the scattering length (and effective range) can be determined, something that is often important in the study of astrophysical reactions. This method has recently been used to study the thermal capture of neutrons by ^{3}He, a very interesting reaction in that it is dominated by two-body currents.[24] The impulse approximation (one-body currents only) would give a zero cross section for this reaction in the absence of the tensor force due to a pseudo-orthogonality condition. Even with the fairly strong tensor force in the Argonne V14 + TNI 7 model, we find that the impulse approximation gives only $\approx 10\%$ of the measured cross section. These same methods are currently being used to study the weak-capture reaction in the four-body system.[25] This reaction produces the highest-energy end-point neutrinos from the sun, and it might be feasible to distinguish their contribution to the total flux in future solar neutrino observatories.

I have described these methods in terms of a one-channel problem. In principle they can also be applied to many-channel problems, in which case one specifies the boundary conditions in all channels. The solutions thus obtained are called eigenphase solutions, and are characterized by the

to experimental situations). By determining several independent solutions at each energy, the full S-matrix can be extracted. This method should be practical for simple interaction models where the variational calculations themselves are rather straightforward, but whether it is practical for realistic problems remains to be seen.

Each of these methods can be employed in GFMC calculations as well. A node in the scattering wave function can be specified by using the well-known image method for the Green's function. The same idea can be used when fixing the logarithmic derivative; one must simply incorporate the flux entering the internal region from the scattering wave function outside the box. By setting the magnitude of the image as well as its distance from the box surface, it is possible to guarantee that the wave function at the surface has a specific logarithmic derivative. GFMC scattering calculations are currently being undertaken for ^{5}He in order to verify or disprove the results of the variational calculations.

GFMC and Flux-Tube Quark Models

Another area in nuclear physics where Monte Carlo methods are valuable is the study of constituent quark models. These models are designed to study some of the basic features of full QCD with a limited number of degrees of freedom. It is hoped that we will be able to understand some of the behaviour of the underlying field theory with these models, in particular to study the rich spectral properties of mesons and baryons and also the nature of confinement.

Of course, lattice QCD algorithms are steadily progressing; they are described elsewhere in this volume. It may be possible in the fairly near future to understand some vital features of QCD, for example the lowest-lying hadronic masses, from first-principles calculations of the field theory. Nevertheless, simple phenomenological quark models may prove useful in understanding the structure and excitation properties of hadrons.

In particular, we examine flux-tube quark models based upon the strong-coupling limit of QCD. In the past, these models have been used to describe the meson and baryon spectra;[26,27] they produce spectra which are generally in good agreement with experiment. Here, we review recent work on the so-called 'exotic' states in the flux-tube model; states composed primary of other than $q\bar{q}$ pairs or qqq triplets. Predictions of bound exotic states abound, the most famous being the H-particle originally proposed by Jaffe,[28] a six-quark state composed of u, d, and s quarks. The nature of confinement plays a vital role in these calculations.

Predictions of the H and other exotics must, to some extent, be influenced by the assumptions inherent in the various models. In particular, a mean-field type of approximation is inherent in the confinement picture of many models.[28-32] including bag models. Here, we study multi-quark hadrons (MQH) having $2q - 2q$, $4q - q$, and $6q$ states in a flux-tube model with quite a different confinement mechanism. These 'exotic' multi-quark states have not previously been calculated within this model.

In the flux-tube quark model it is assumed that the color electric flux is confined to narrow, stringlike tubes joining the quarks. A flux tube starts from every quark i and ends on an antiquark i. and three flux-tubes i,j,k can end or start from an anti-symmetric ϵ_{ijk} junction called the Y-junction. The resulting flux-tube patterns for the familiar $q\bar{q}$ and $3q$ states, as well as the exotic

MQH having four to six particles are shown in figure 6. As is apparent in the figure, a state with N+1 particles is generated by replacing a quark or an antiquark in an N particle state by a Y-junction and two anti-quarks or quarks.
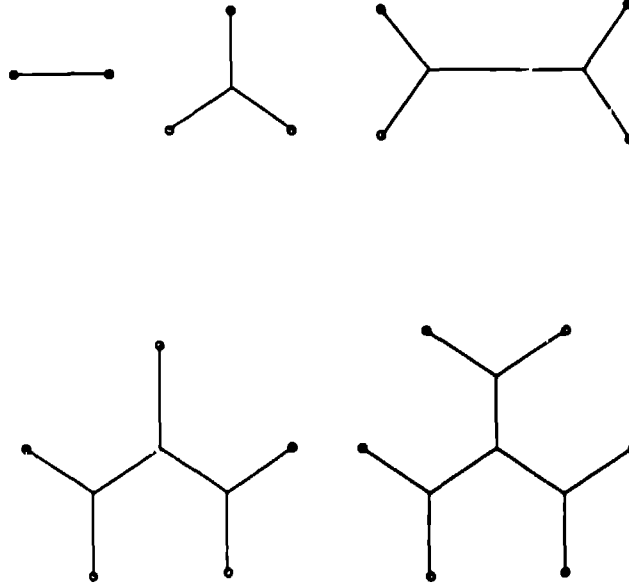

Figure 6) Possible flux tube configurations states of 2 to 6 quarks.

The quarks are treated as semi-relativistic spin 1/2 Pauli particles. In contrast, bag[28-31] and other mean-field[32,33] models treat quarks more accurately as relativistic Dirac spinors. We solve for eigenstates of a Hamiltonian H_Q with three terms involving only quark degrees of freedom:

$$H_Q = H_0 + H_F + H_I, \tag{20}$$

where H_0 is the relativistic kinetic energy of the quarks:

$$H_0 = \sum_{i=1,N} (m_i^2 + p_i^2)^{1/2}. \tag{21}$$

The confining interaction H_F represents the energy of the flux tubes. L is obtained by minimizing the total length of the tubes for any given position of the Y-junctions. If L is the minimum length for a configuration $\{r_i, i = 1, N\}$ of the quarks, the energy is:

$$H_F = \sqrt{\sigma} L(r_i) - N\delta M. \tag{22}$$

The factor $\sqrt{\sigma}$ is the string tension of the tubes and δM is a constant term. When fitting mesons and baryons, this constant appears to be proportional to N, hence it is natural to associate them with the free ends of the tubes.

H_I represents the short range one gluon exchange interaction between the quarks. It consists of a Coulomb, spin-spin, tensor, and spin-orbit terms. Our primary interest here is in low-energy S-wave hadrons in which the tensor and spin-orbit interactions are not very important. Hence, for the sake of simplicity, we use

$$H_I = \alpha \sum \sum F_i^a F_j^a \{ \frac{1}{r_{ij}} - \frac{2\pi}{3m^2} s(r_{ij}) \sigma_i \cdot \sigma_j \}. \tag{23}$$

Here F_i^α is $1/2\lambda_i^\alpha$ for quarks and $-1/2(\lambda_i^\alpha)^*$ for antiquarks, and α_c is the QCD fine structure constant. The usual δ function in the spin-spin interaction is broadened by assuming $\exp(-\frac{1}{2}\Lambda^2 q^2)$ vertex form factors, so that

$$s(r) = (\frac{2}{\sqrt{\pi}\Lambda})^3 \exp(-\frac{r^2}{4\Lambda^2}). \tag{24}$$

The interaction parameters used are obtained by fitting the masses of light mesons and baryons.[27]

The interpretation of this model is trivial for $q\bar{q}$ and $3q$ states, however things are not as simple for $N \geq 4$. Three different flux-tube arrangements are possible for the $2q - 2\bar{q}$ state, as shown in figure 7. Even when the quark positions are the same, in the extreme strong-coupling limit the states $|I\rangle$, $|II\rangle$, and $|III\rangle$ are orthogonal to each other due to differences in the link operators (flux tubes). They have different flux topologies, and hence are not coupled by the Hamiltonian H_Q.
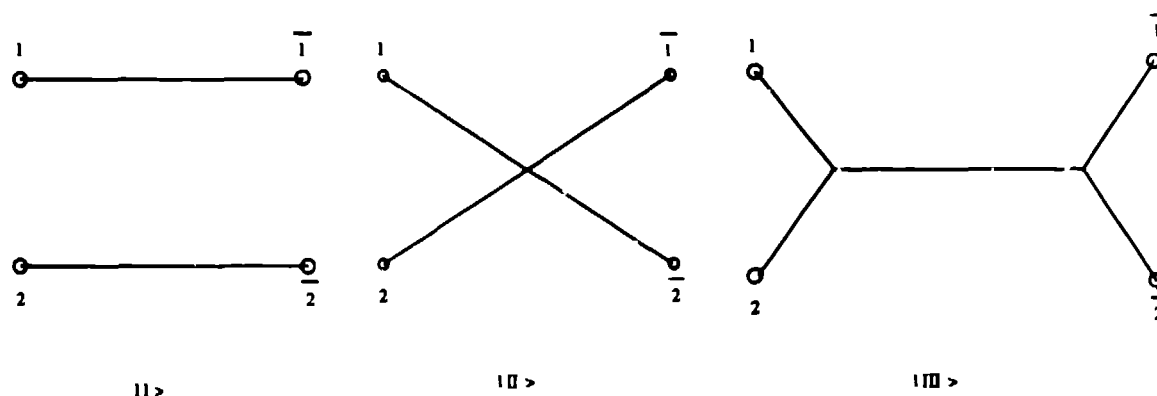

Figure 7) The three flux tube configurations for $2q - 2\bar{q}$ states.

Of course a more realistic QCD Hamiltonian would have other terms in addition to H_Q. One such term is a string-breaking term which couples states with different numbers of particles. Models for this term have been used to study the decay of mesons into two mesons,[34] the meson-baryon couplings,[35,36] and the $\Delta \to N + \pi$ width.[37] It gives second-order corrections to the hadron energies[37] which can partly be absorbed into the values of the parameters $\sqrt{\sigma}$ and δM. H_B can couple the four-quark states $|I\rangle$ and $|II\rangle$ in 4th order. It cannot change the number of Y-junctions, and hence does not couple $|III\rangle$ to either $|I\rangle$ or $|II\rangle$.

There should also be a term which creates or destroys closed plaquettes of flux tubes; this term can create or annihiliate Y-junctions. The effect of this term on hadron spectroscopy has not been studied. In the limit that the quark mass is large one can take the point of view that these terms can change the flux topology faster than the motion of the quarks. In this limit one may be able to use the topology that gives the lowest H_F for a given configuration of quarks, as has been assumed in some models.[38] In the present work we assume that for light quarks it is more reasonable to start with H_Q and treat effects of H_B and H_P perturbatively.

There are also some novel anti-symmetry requirements imposed by this Hamiltonian. Obviously, a specific configuration of flux-tubes; for example quarks (1,2), (3,4), and (5,6) paired together within Y-junctions in a $6q$ state; does not describe a fully symmetric Hamiltonian. In fact, in strong coupling QCD states with different pairings are in general orthogonal to each other by the same arguments given above. Thus, there is no special anti-symmetry required between quarks in

different pairs, or for that matter between different baryons.[39-42] However, we must anti-symmetry between quarks connected to the same Y-junction, and also must respect the symmetry when pairs of quarks are exchanged.

Quark Model Calculations

We have studied the MQH states in the flux-tube model with both Variational Monte Carlo (VMC)[26,27] and Green's Function Monte Carlo (GFMC)[44] methods. For the most part, the algorithms are very similar to those used to study light nuclei, here I only briefly discuss the variational wave functions and the few novel techniques required.

Our choice of variational (trial) wave functions for the 'exotic' hadrons (states in which all quarks are confined into one region by flux tubes) was guided by previous studies of the mesons and baryons. Initially, we consider only the lowest-energy spatial wave function, determining the lowest state of the spin-independent Hamiltonian; the sum of kinetic, flux-tube and color coulomb energies. The symmetry requirements can then be satisfied by an appropriate choice of spin-flavor wave functions. For the $2q - 2\bar{q}$ system, the spatial part of the wave function Ψ_T is:

$$\Psi_T = f(r_{12})f(r_{34})F(R_{12}, R_{34}) \tag{25}$$

where particles 1 and 2 are quarks and 3 and 4 are anti-quarks. The f_{ij} are functions of the distance between particles i and j, and have the same functional form used previously in the meson and baryon studies:

$$f(r) = r^\delta \exp[-w(r)(\gamma_1 r + \gamma_2 r^2) - (1 - w(r))\gamma_{1.5}r^{1.5}]. \tag{26}$$

The factors γ and the constant δ are variational parameters, and $w(r)$ is a Woods-Saxon function whose strength and range are additional variation parameters. This form interpolates between a Coulomb-like solution near the origin to the behavior appropriate to a linear potential at large separations. The function F describes correlations between the center-of-mass of the quarks (1&2) and the anti-quarks (3&4), and it is chosen as:

$$F(R) = \exp[-\gamma_c R^{1.5}]. \tag{27}$$

The constant γ_c is an additional variational parameter.

The spatial part of the trial functions for the other systems are similar; pair correlations between quarks attached to the same Y-junction are multiplied by correlations between the central junctions themselves. For example, the six-quark wave function is given by

$$\Psi_T = f(r_{12})f(r_{34})f(r_{56})F(R_{12}, R_{34})F(R_{12}, R_{56})F(R_{34}, R_{56})[1 - \beta V_3(R_{12}, R_{34}, R_{56})]. \tag{28}$$

The quarks 12, 34, and 56 are paired in this wavefunction, and we use the same form for the two-body correlations f and the pair center-of-mass correlations F as in the $2q - 2\bar{q}$ case. The last term in this expression is a small three-body correlation between the centers-of-mass of the pairs, its functional form is the same as the three body correlations used previously in studies of the

non-pairwise components of the six-body potential into the trial wave function. These variational wave functions give accurate energies for the ground states of the spin-indepdnent Hamiltonian, typically within nearly one standard error (~ 20 MeV) of the exact GFMC result.

I will not describe the spin-flavor parts of the wave functions here, they are presented in detail in reference 43. I merely note that it is energetically favorable to couple quarks paired to the same Y-junction to a total spin 0; these quarks are more strongly correlated by the confining interaction, hence they are most affected by the hyperfine interaction. For example, in the H-dibaryon all the paired quarks can be coupled to spin 0, giving a more attractive hyperfine interaction than is present in two isolated baryons.

Evaluating the two-body potential terms is straightforward using traditional Monte Carlo methods; the many-body confining interaction is only slightly more complicated. For example, given a specific set of quark coordinates in the six-quark state; we guess the position of the central Y-junction (figure 6). The position of the remaining Y-junctions then be determined algebraically using the formulas given in reference 26. The remaining task is to minimize the total length by varying the position of the central Y-junction. The simplex method works quite well here, and typically requires of the order of 10 iterations to provide a very accurate potential energy.

We also need to evaluate the propagator for the semi-relativistic kinetic energy operator, as well as devising a method for evaluating the kinetic energy in a variational calculation. This operator involves all powers of the momentum; hence the free-particle propagator

$$\langle \Psi_T | \exp(-\sqrt{(p_i^2 + m_i^2)}\Delta\tau) | \Psi_T \rangle \tag{29}$$

is non-local in character. The free particle propagator is given in reference 44 :

$$G(R) = \frac{4\pi}{2\pi^3}\frac{\beta\alpha^2}{R^3(1 + \beta^2)}K_2[\alpha(1 + \beta^2)^{1/2}], \tag{30}$$

with

$$\begin{aligned}\beta &= \frac{\hbar c\Delta\tau}{R} \\ \alpha &= mcR/\hbar.\end{aligned} \tag{31}$$

The propagation distance is R, and K_2 is a Bessel function of order two. This propagator has a long-distance tail that decays with the Compton wavelength of the particle. The rate of decay is independent of time step, but the amplitude of the tail is proportional to $\Delta\tau$. In the long-time (low-momentum) limit, it coincides with the non-relativistic propagator, as expected. The semi-relativistic propagator is only slightly more difficult to sample than the gaussians used in non-relativistic calculations. When calculating the expectation value of the kinetic energy, it is possible to determine the propagator terms linear in $\Delta\tau$ analytically, and hence sample the kinetic energy without introducing any approximations.

The spin-independent Hamiltonian contributes the dominant terms in the energy, therefore we initially consider the results for this simplified Hamiltonian. The results are summarized in figure 8, their most striking feature is that each additional particle added to the system raises the energy by a roughly constant amount. The additive constant is large (~ 540 MeV), and hence the exotic MQII states are four to five hundred MeV higher than states composed of two isolated hadrons.

This is not a trivial result since for some configurations of the particles the MQH confining potential is less repulsive than for two isolated baryons. Overall, however, in the flux tube model it costs more kinetic and potential energy to form the multi-quark systems. It is amusing to note that exactly the same additive effect would be predicted in simple the simple di-quark picture.
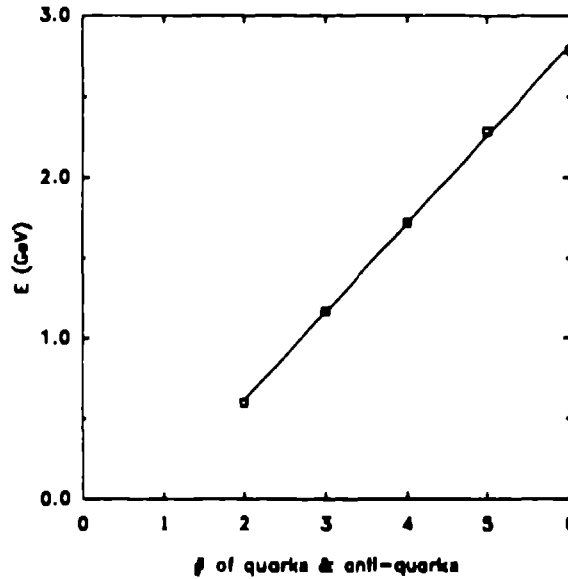

Figure 8) Lowest single-hadron energy vs. number of quarks and anti-quarks.

Of course, the hyperfine interaction must be included in any reasonable calculation. The strength of the hyperfine interaction has been adjusted to roughly reproduce the experimental $N - \Delta$ splitting of ~ 290 MeV; with these parameters we obtain a splitting of .27 GeV. Other effects, including coupling to pions (string-breaking) may also contribute ~ 0.1 GeV to this split-ting.[37] This model reproduces the experimental $\pi - \rho$ splitting of 630 MeV, however the pion has a rather small energy of 55 MeV.

Consider the six quark systems; both the S=0 H dibaryon and a proposed S=3 exotic six-quark state. In the latter, of course, the hyperfine interaction is repulsive. However, if the six-quark state is larger in spatial extent than the spin 3/2 baryon, the hyperfine interaction may be less repulsive. Hence, this state is a possible candidate for a bound exotic. The results for these systems are given in Table 1.

Table 1: Energies of Six-Quark States

State	Energy (GeV)
2x N	2.00
$6q(S = 0)$	2.30
2x Δ	2.54
$6q(S = 3)$	2.90

Green's function Monte Carlo results for the two hadron and MQH 6 quark states with the full interaction, assuming SU3 symmetry.

We have computed the H dibaryon in the SU3 limit in which all u, d, and s quarks have the same mass. The hyperfine interaction does provide a relative attraction for the H dibaryon when compared to two baryons. Two isolated spin 1/2 baryons gain approximately 350 MeV from the spin-dependent term, while the H dibaryon gains $\sim$ 500 MeV. This shift is close to what one would expect from first order perturbation theory. The 3q baryons have one S=0 pair each, thus their total energy shift is roughly equal to the $N - \Delta$ splitting. The H-dibaryon has three such pairs, and consequently gains an energy of nearly 1.5 times the $N - \Delta$ splitting. However, this additional attraction is not nearly strong enough to overcome the much higher energy of the 6-quark state in the confining potential; indeed the full calculation reveals that the energy difference between the H and two baryon states is 300 MeV in the SU3 limit. Including the affects of a larger strange quark mass only increases the mass of the H relative to the two isolated baryons.

Next, consider the proposed S=3 dibaryon. In this case the two isolated baryons (Δs) are pushed up approximately 200 MeV by the hyperfine interaction. This shift is somewhat smaller than that of two nucleons due to non-perturbative effects in the nucleon channel.[27] The energy shift in the six-quark state ($\sim$ 190 MeV) is only slightly smaller. Consequently, the six-quark state again remains higher in energy than two baryons, this time by approximately 450 MeV. Mean-field models typically produce a six-quark state of significantly larger spatial extent than baryons; and hence a smaller hyperfine repulsion in the spin 3 dibaryon. This effect is very small in the present model; here the results are dominated by the spin-independent interaction.

Results in the 2q – 2$\bar{q}$ and 4q – $\bar{q}$ systems are similar. The spin 0 four-quark state is very high in energy compared to two pions; as expected, since the pions feel an extraordinarily strong hyperfine interaction. We would also predict no strong spin-2 exotic resonance with the flux tube model. We do not expect these MQH states to exist as sharp resonances at high energy. We have explored an extreme limit of the theory in order to better understand the possible range of quark models. In this limit there is no coupling between the MQH and multi-hadron states. Physically the H$_P$ (neglected in this work) provides this coupling, and thus all MQH states will have a width. Unfortunately, since H_P is largely unknown, we cannot provide any reliable estimate of the widths. This term in the Hamiltonian is an important topic for future study.

In summary, we find that in the limit of weak coupling between different flux-tube configurations there are no bound multi-quark states. Our results stand in sharp contrast to mean-field models which explain traditional meson and baryon spectroscopy with a similar degree of accuracy. They also differ considerably from two-body potential based quark models, in which the hyperfine interaction provides enough attraction to produce sharp low-energy resonances in certain spin-isospin channels. Consequently, the presence or absence of these exotic states in the experimental spectrum may be an important guide in our understanding of QCD.

Outlook

Monte Carlo methods provide a valuable tool for understanding the properties of few-body systems in nuclear physics. Due to the complexities of nuclear interactions, these methods have not been exploited to the degree they have in other fields of physics. Nevertheless, Monte Carlo methods have a wide range of applicability, including the study of very light nuclei, quark models.

and also hypernuclear physics.

With the help of these methods, we have developed a coherent picture of the structure and static electromagnetic properties of light nuclei. These rather traditional models depend upon three-nucleon-interactions and the presence of exchange currents. They are also being employed to study correlations within the nucleus, as well as low-energy reactions of astrophysical interest.

Many important challenges lie ahead, of course. Foremost among these are calculations of larger nuclei and development of new techniques for treating the dynamic properties of nuclei. Heavier nuclei offer the opportunity for studying very neutron-rich nuclei, which are important astrophysically through their connection with neutron stars. A better understanding of current and future electron scattering experiments requires reliable calculations of the dynamic response of nuclei, perhaps the most challenging goal for Monte Carlo (or any other) methods.

References

1. M. H. Kalos, Phys. Rev. **128** 1791 (1962).

2. J. Lomnitz Adler, V. R. Pandharipande, and R. A. Smith, Nucl. Phys. **A315** 399 (1981).

3. M. H. Kalos, D. Levesque, and L. Verlet, Phys. Rev. **A9** 2178 (1974).

4. J. Carlson, Phys. Rev. **C36**, 2026 (1987), Phys. Rev. **C38** 1879 (1988).

5. M. H. Kalos, M. A. Lee, P. A. Whitlock and G. V. Chester, Phys. Rev. **B24** 115 (1981).

6. R. M. Panoff and J. Carlson, Phys. Rev. Lett. **62** (1989) 1130 (1989).

7. R. B. Wiringa, R. A. Smith, and T. L. Ainsworth, Phys. Rev. **C29** 1207 (1984).

8. R. Machleidt, K. Jolinde, and Ch. Elster, Phys. Rep. **149** 1 (1987).

9. M. M. Nagles, T. A. Rijken, and J. J. de Swart, Phys. Rev. **D17** 768 (1978).

10. J. Carlson, V. R. Pandharipande, and R. B. Wiringa, Nucl. Phys. **A401**, 59 (1983).

11. R. Schiavilla and D. O. Riska, University of Helsinki preprint HU-TFT-90-15.

12. R. B. Wiringa (to be published).

13. J. Carlson, Nucl. Phys. **A508** 141c (1990).

14. D. M. Ceperley and E. L. Pollock, Phys. Rev. Lett. **56** 351 (1986).

15. J. Carlson (to be published).

16. G. L. Payne, private communication.

17. D. O. Riska, Physica Scripta **31**, 471 (1985).

18. R. Schiavilla, V. R. Pandharipande, and D. O. Riska, Phys. Rev. **C41** 309 (1990).

19. W. Kloet and J. Tjon, Phys. Lett. **49B** 419 (1974).

20. R. Schiavilla, et al., Nucl. Phys. **A473** 317 (1987).

21. R. Schiavilla, V. R. Pandharipande, and A. Fabrocin, Phys. Rev. **C40** 1484 (1989).

22. D. H. Beck, Phys. Rev. Lett. **64** 268 (1990).

23. J. Carlson, K. E. Schmidt, and M. H. Kalos, Phys. Rev. **C36**, 27 (1987).

24. J. Carlson, D. O. Riska, R. Schiavilla, and R. B. Wiringa, Phys. Rev. **C42** 830 (1990).

25. J. Carlson, D. O. Riska, R. Schiavilla, and R. B. Wiringa, Los Alamos preprint (1990).

26. J. Carlson, J. Kogut, and V. R. Pandharipande, Phys. Rev. **D28**, 2807 (1983).

27. J. Carlson, J. Kogut, and V. R. Pandharipande, Phys. Rev. **D27**, 233 (1983).

28. R. L. Jaffe, Phys. Rev. Lett. **38**, 195 (1977); **38**, 617(E) (1977).

29. Th. M. Aerts, P. J. G. Mulders, J. J. deSwart, Phys. Rev. **D17**, 260 (1978).

30. P. J. G. Mulders and A. W. Thomas, J. Phys. **G9**, 1159 (1983).

31. K. Saito, Prog. Theor. Phys. **72**, 674 (1984).

32. T. Goldman, G. J. Stephenson, K. E. Schmidt, Fan Wang, Phys. Rev. **C39**, 1889 (1989).

33. T. Goldman, et al., Phys. Rev. Lett. **59**, 627 (1987); Nucl. Phys. **A481**, 621 (1988).

34. S. Kumano and V. R. Pandharipande, Phys. Rev. **D38**, 146 (1988).

35. F. Stancu and P. Strassart, Phys. Rev. **D38**, 233 (1988); Phys. Rev. **D39**, 39 (1989).

36. G. A. Miller, Phys. Rev. **C39**, 1563 (1989).

37. S. Kumano, Phys. Rev. **D[41**, 195 (1990).

38. S. Gardner and E. J. Moniz, Phys. Rev. **C36**, 2504 (1987).

39. N. Isgur and J. Paton, Phys. Rev. **D31**, 2910 (1985).

40. N. Isgur, Nucl. Phys. **A497**, 91c (1989).

41. G. A. Miller, Nucl. Phys. **A497**, 277c (1989).

42. John Merlin and Jack Paton, J. Phys. **G11**, 439 (1985).

43. J. Carlson and V. R. Pandharipande, Los Alamos preprint LA-UR-90-2088 (to appear in Phys. Rev. **D**).

44. J. Carlson, L. Heller, and T. Tjon, Phys. Rev.**D37**, 744 (1988).